JACS
JOURNAL OF THE AMERICAN CHEMICAL SOCIETY

Communication

pubs.acs.org/JACS

High and Reversible Ammonia Uptake in Mesoporous Azolate Metal–Organic Frameworks with Open Mn, Co, and Ni Sites

Adam J. Rieth,[†] Yuri Tulchinsky,[†] and Mircea Dincă*

Department of Chemistry, Massachusetts Institute of Technology, 77 Massachusetts Avenue, Cambridge, Massachusetts 02139, United States

Supporting Information

ABSTRACT: A series of new mesoporous metal–organic frameworks (MOFs) made from extended bisbenzenetriazolate linkers exhibit coordinatively unsaturated metal sites that are responsible for high and reversible uptake of ammonia. Isostructural Mn, Co, and Ni materials adsorb 15.47, 12.00, and 12.02 mmol of NH_3/g, respectively, at STP. Importantly, these near-record capacities are reversible for at least three cycles. These results demonstrate that azolate MOFs are sufficiently thermally and chemically stable to find uses in recyclable sorption, storage, and potentially separation of chemically challenging and/or corrosive gases, especially when designed to exhibit a high density of open metal sites.

Among industrial gases that are produced and used on a large scale, ammonia is one of the most corrosive and toxic. Its containment through sorption is thus essential for industrial air remediation[1] or in gas masks as a surrogate for sorption of chemical warfare agents.[2,3] Despite its corrosiveness and toxicity, it is also widely used as a heat exchange fluid both in conventional compression-based heat pumps and in thermal batteries or adsorption heat pumps, which have the potential to transform the HVAC market.[4,5] In these applications, ammonia must be adsorbed at very low pressures or low relative concentrations. This requires that adsorbents interact with ammonia very strongly through chemisorption interactions that generate a high enthalpy of adsorption. State-of-the-art sorbents currently used for commercial and industrial applications, activated carbons, suffer from low affinities as well as low capacities of less than 11 mmol g^{-1}.[5,6]

Because of their record porosity and chemical tunability, metal–organic frameworks (MOFs) have the potential to greatly surpass the capacities and affinities of current sorbents. MOFs formed with carboxylate ligands and containing open metal sites, including HKUST-1 (Cu_3BTC_2, H_3BTC = benzene-1,3,5-tricarboxylic acid) and Cu-MOF-74 (Cu_2DOBDC, H_4DOBDC = 2,5-dihydroxy-1,4-benzenedicarboxylic acid), have been explored as ammonia sorbents.[7,8] However, both HKUST-1 (ammonia uptake of 13 mmol g^{-1} at STP) and Cu-MOF-74 lose crystallinity and porosity upon contact with ammonia gas.[7,8] Covalent organic frameworks (COFs) have also been explored as ammonia sorbents. COF-10, a two-dimensional honeycomb structure with boronic ester linkages, has a relatively high reversible capacity of 10.8 mmol g^{-1} at STP, with slow degradation upon cycling.[9] BPP-5, a carboxylate-functionalized interpenetrated diamondoid porous organic polymer, has an extremely high ammonia capacity of 17.7 mmol g^{-1} at STP.[10] However, the interpenetrated nature of BPP-5 gives it small pores that significantly impede the sorption kinetics, making reversibility impractical.[10] Slow sorption limits the utility of a sorbent by increasing the pressure drop in applications such as gas masks and limits the cycling rate and implicitly the cooling power in adsorption heat pumps.[11] Most recently, it was shown that Prussian blue analogues also exhibit very high ammonia uptake, some reversibly.[12] These examples notwithstanding, the development of tunable, high-capacity ammonia sorbents that can chemically withstand multiple adsorption/desorption cycles would clearly impact many branches of industry that rely on this important feedstock chemical.

MOFs with azolate linkers, such as pyrazolate, imidazolate, and triazolate, have greatly enhanced stability toward polar coordinating solvents due to the greater Lewis basicity of azolate anions versus carboxylates.[13−16] We surmised that introducing coordinatively unsaturated metal sites in mesoporous azolate MOFs would provide materials that could adsorb ammonia without collapsing, in contrast to carboxylate-based MOFs with open metal sites, with the mesoporosity also allowing faster sorption kinetics for practical applications. Here we describe the synthesis and ammonia sorption properties of the first azolate-based MOFs that exhibit mesoporous channels. Coordinatively unsaturated metal sites that line the pores of these new materials contribute to near-record reversible ammonia sorption.

Inspiration for the design of the new ammonia sorbents came from a recent report of M_2Cl_2BBTA (H_2BBTA = 1*H*,5*H*-benzo(1,2-*d*:4,5-*d*′)bistriazole; M = Co, Mn),[17] a material that exhibits open metal sites lining 11 Å-wide pores in a non-interpenetrating topology. Seeking to expand this structure isoreticularly into the mesoporous regime in a manner akin to the IRMOF-74 series,[18] we employed an extended bisbenzotriazole ligand, bis(1*H*-1,2,3-triazolo[4,5-*b*],[4′,5′-*i*])dibenzo-[1,4]dioxin (H_2BTDD).[19] Treatment of H_2BTDD with hydrated divalent metal chlorides in *N*,*N*-dimethylformamide (DMF), an alcohol cosolvent, and a small amount of hydrochloric acid (HCl) at 65 °C afforded $Mn_2Cl_2(BTDD)(H_2O)_2$ (**1**), $Co_2Cl_2(BTDD)(H_2O)_2$ (**2**), and $Ni_2Cl_2(BTDD)(H_2O)_2$ (**3**) as crystalline powders solvated with various amounts of DMF, water, and/or alcohol guest molecules. X-

Received: June 4, 2016
Published: July 15, 2016

DOI: 10.1021/jacs.6b05723
J. Am. Chem. Soc. 2016, 138, 9401−9404

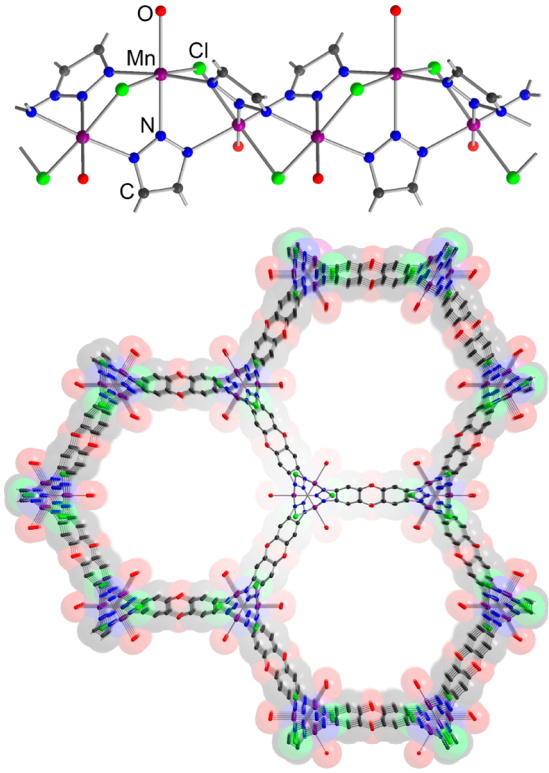

Figure 1. Single-crystal X-ray structure of **1**. (top) The secondary building unit viewed along the *c* axis. (bottom) View down the *c* axis.

ray diffraction analysis of a single crystal of **1** revealed a structure consisting of a three-dimensional lattice displaying a honeycomb network along the *c* direction, analogous to the M_2Cl_2BBTA materials (Figure 1).[17] Each Mn ion is coordinated by three nitrogen atoms from three separate $BTDD^{2-}$ linkers, two bridging chlorides, and a terminal water molecule pointing toward the interior of the ∼22 Å-wide mesopores. The secondary building units consist of one-dimensional (1D) chains formed by Mn ions and bridging triazolate and chloride ligands (Figure 1). Although we were able to isolate **2** and **3** only as microcrystalline powders, powder X-ray diffraction revealed these to be isostructural to **1**, both as-synthesized and after activation (Figures S1 and S2).

Thermogravimetric analysis (TGA) of all three materials showed similar mass losses between approximately 50 and 150 °C followed by a precipitous decline in mass at 450 °C (Figure S3). These may be attributed to loss of guest and bound solvent molecules and framework decomposition, respectively. The loss of bound solvent molecules should generate one open coordination site per metal center, as has been observed for the narrow-pore analogue M_2Cl_2BBTA[17] as well as IRMOF-74 materials, which bear analogous structures.[20,21] Exchanging bound solvent molecules in the as-synthesized materials with methanol through Soxhlet extraction followed by activation at 100 °C under dynamic vacuum provided dry materials $M_2Cl_2(BTDD)$ (M = Mn, Co, Ni), as confirmed by elemental analysis (see the Supporting Information). Upon activation, color changes from red to green and from white to lime-green are observed for **2** and **3**, respectively, consistent with the expected change in the metal ion coordination number from six to five. Unremarkably for Mn^{2+} compounds, **1** remains off-white upon activation. Nitrogen adsorption isotherms at 77 K for activated samples of **1**, **2**, and **3** exhibit type IV isotherms,

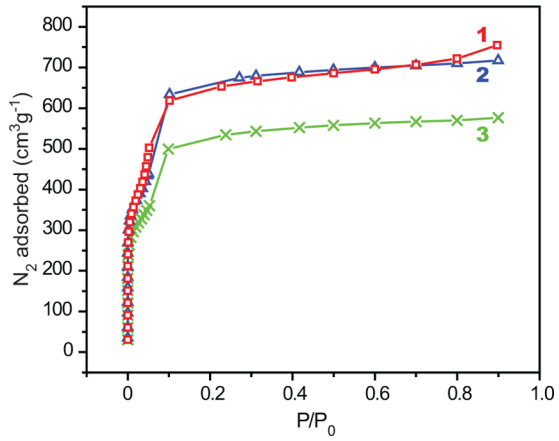

Figure 2. N_2 adsorption isotherms (77 K) for activated samples of **1** (red squares), **2** (blue triangles), and **3** (green crosses).

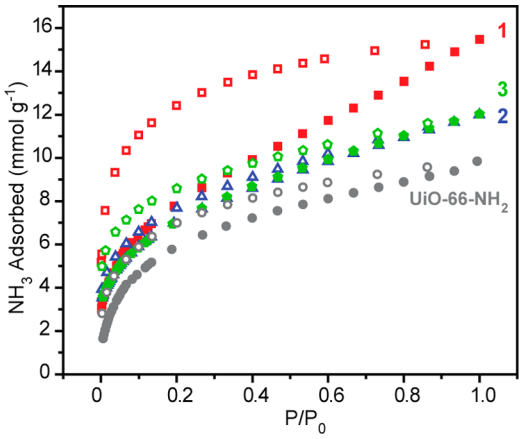

Figure 3. NH_3 adsorption (solid symbols) and desorption (open symbols) at 1 bar, 298 K for activated samples of **1** (red squares), **2** (blue triangles), **3** (green pentagons), and UiO-66-NH_2 (gray circles).

characteristic of mesoporous structures. Fitting the appropriate[22] portion of each isotherm to the Brunauer–Emmett–Teller (BET) equation[23] gave apparent BET areas of 1917, 1912, and 1762 $m^2\ g^{-1}$ for activated **1**, **2**, and **3**, respectively (Figure 2 and Table S2). Barrett–Joyner–Halenda (BJH) pore size distribution analysis[24] using the Kruk–Jaroniec–Sayari[25] correction for hexagonal pores indicated narrow pore size distributions centered at 21.4 Å for **1**, **2**, and **3** (Figure S4), in line with the pore width expected from the crystal structure of **1** (ca. 22 Å).

To test our materials for ammonia sorption and compare them with established results, we also analyzed a sample of UiO-66-NH_2,[26] which has received considerable attention for applications in ammonia sorption.[1,2,27] Ammonia adsorption experiments for activated **1**, **2**, and **3** all revealed type I isotherms, with sharp uptakes at low absolute pressure and total uptakes of 15.47, 12.00, and 12.02 mmol g^{-1} for **1**, **2**, and **3**, respectively, at 1 bar and 298 K (Figure 3). Importantly, the high ammonia uptakes are reversible over at least three cycles (Figure 4). In contrast, although the carboxylate-based UiO-66-NH_2 showed an uptake of 9.84 mmol g^{-1} in the first cycle, in line with previous reports,[10,27] it nevertheless exhibited significant loss of crystallinity and lost more than 50% of its initial capacity after three consecutive cycles of ammonia sorption (Figures 4 and S5).

DOI: 10.1021/jacs.6b05723
J. Am. Chem. Soc. 2016, 138, 9401–9404

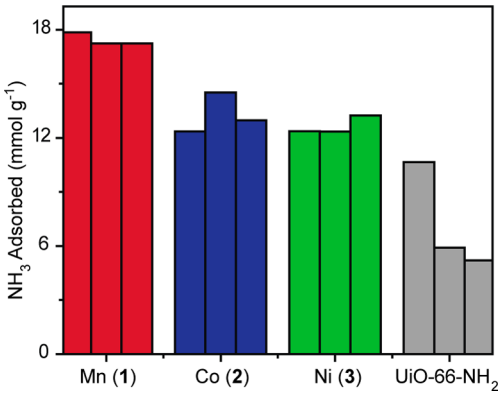

Figure 4. Uptake data for NH_3 adsorption at 1 bar, 293 K for activated samples of **1** (red), **2** (blue), **3** (green), and UiO-66-NH_2 (gray). Bars represent iterative cycles on the same sample of each material.

Ammonia uptake isotherms were also measured at 293 and 283 K, temperatures that are relevant for cooling applications.[4] The total uptakes at 1 bar were 17.86 and 22.43 mmol g^{-1} for **1**, 12.36 and 16.24 mmol g^{-1} for **2**, and 12.37 and 16.58 mmol g^{-1} for **3** at 293 and 283 K, respectively (Table S3 and Figure S6). Regardless of the adsorption temperature, the desorption curves were invariably hysteretic. Thus, during desorption at 298, 293, or 283 K, all three materials exhibit pronounced hysteresis terminating with respective uptakes of 9.35, 4.15, and 4.43 mmol g^{-1} for **1**, **2**, and **3**. Importantly, the expected uptake values upon adsorption of one molecule of NH_3 per metal site (i.e., two NH_3 molecules per formula unit of $M_2Cl_2(BTDD)$) for **1**, **2**, and **3** are 4.50, 4.42, and 4.43 mmol g^{-1}, respectively. These are very close to the low-pressure desorption values observed for **2** and **3**, suggesting that indeed the first NH_3 molecule adsorbs very strongly to the Co and Ni open sites in these materials. These bound ammonia molecules can be fully removed upon heating the materials at 200 °C under dynamic vacuum. TGA–MS data indicate that the materials indeed desorb ammonia at approximately 150 °C (Figure S7). Binding of ammonia to the metal centers is also supported by elemental analyses of samples isolated upon desorption (before full recycling at 200 °C), which matched the formulas $Mn_2Cl_2BTDD\cdot(NH_3)_{1.7}\cdot(MeOH)_{2.3}$ for **1**, $Co_2Cl_2BTDD\cdot(NH_3)_{1.9}$ for **2**, and $Ni_2Cl_2BTDD\cdot(NH_3)_{2.2}$ for **3** (see the Supporting Information). Finally, upon ammonia uptake, activated **2** and **3** returned to their original red and white colors, indicative of saturated Co and Ni ions, respectively.

Surprisingly, the lowest-pressure point on the desorption curve for **1**, 9.35 mmol g^{-1}, corresponds to 2.08 molecules of ammonia per Mn site, double the expected value. This could be due to a structural rearrangement that opens a second coordination site on the Mn ions, as enabled by the chloride bridging ligands becoming terminal, for instance. To this end, we note that powder X-ray diffraction of **1**, **2**, and **3** after ammonia cycling indicates virtually no loss in crystallinity for **2** and **3** but a reduction of diffraction peak intensity for **1** (Figure S8), again in line with a possible rearrangement. Powder neutron diffraction studies aimed at investigating the nature of the enhanced adsorption at Mn ions are underway. Accompanying the decrease in crystallinity, a lower BET surface area of of 596 m^2 g^{-1} was also measured for **1** from N_2 adsorption isotherms performed after ammonia cycling (Figure S9). Notably, **2** and **3** maintained surface areas of 1843 and 1597 m^2 g^{-1}, respectively, upon ammonia cycling (Figure S9). Despite the relative loss of porosity for **1**, none of the three materials exhibited a decline in ammonia uptake capacity with cycling. Thus, although the BET area decreases, the open metal sites that bind ammonia strongly must still remain accessible. Similar behavior was observed in COF-10, where, although the nitrogen uptake at 77 K declined approximately 60% after three cycles, the ammonia capacity declined only 4.5%. This discrepancy was attributed to the Lewis acidic boron centers remaining accessible to ammonia.[9] Our observations therefore confirm previous observations that a decrease in BET area is not predictive of a decline in ammonia uptake; rather, the strength of interaction between the material and ammonia is a better predictor of the overall uptake.[9,10]

To gain insight into the strength of ammonia binding in each material, we fit the 283 and 293 K isotherms independently using the dual-site Langmuir–Freundlich equation (Figure S6).[28] On the basis of these fits, isosteric heats of adsorption were calculated using the Clausius–Clayperon equation (Figure S10). Although this method gives reliable "zero-coverage" heats of adsorption for physisorptive interactions, we found that in this case extrapolation to zero coverage gave unreasonable fits and heat of adsorption values. This is not surprising because the assumptions underlying Clausius–Clapeyron thermodynamics include reversibility, which is not observed in our systems. Although challenges related to fitting the isotherms at low coverage may be mitigated by collecting more data points at low pressure, this is impractical because single-pressure points in this region are not reliable and are difficult to measure for strongly interacting adsorptives (Figure S10).

The foregoing results demonstrate ammonia uptake values that are among the highest known for MOFs or organic polymers. Importantly, this work describes the first examples of MOFs with high uptakes that are stable toward repeated cycling of ammonia, advancing the utility of these materials in applications such as trace contaminant removal from air as well as in thermal batteries. The stability of azolate frameworks with open metal sites enables their use in environments with corrosive gases such as power plant flue gas streams. Analogous azolate frameworks with open metal sites may be ideally suited for the capture and separation of other coordinating, Lewis basic, or corrosive analytes.

■ ASSOCIATED CONTENT

Supporting Information

The Supporting Information is available free of charge on the ACS Publications website at DOI: 10.1021/jacs.6b05723.

Synthetic details, physical methods, parameters for calculation of BET area, ammonia uptake data in tabular form, attempted calculation of isosteric heats of adsorption, and Figures S1–S10 (PDF)

Crystallographic data for Mn_2Cl_2BTDD (CIF)

■ AUTHOR INFORMATION

Corresponding Author

*mdinca@mit.edu

Author Contributions

†A.J.R. and Y.T. contributed equally.

Notes

The authors declare no competing financial interest.

DOI: 10.1021/jacs.6b05723
J. Am. Chem. Soc. 2016, 138, 9401–9404

■ ACKNOWLEDGMENTS

This research was supported by the MIT Tata Center for Technology and Design. Fundamental studies of metal−small molecule interactions are supported by a CAREER Award to M.D. from the National Science Foundation (DMR-1452612). M.D. acknowledges the Sloan Foundation, the Research Corporation for Science Advancement (Cottrell Award), and 3M for nontenured faculty funds. We thank Dr. P. Mueller for assistance with crystallography.

■ REFERENCES

(1) Jasuja, H.; Peterson, G. W.; Decoste, J. B.; Browe, M. A.; Walton, K. S. *Chem. Eng. Sci.* **2015**, *124*, 118.
(2) Peterson, G. W.; DeCoste, J. B.; Fatollahi-Fard, F.; Britt, D. K. *Ind. Eng. Chem. Res.* **2014**, *53*, 701.
(3) Britt, D.; Tranchemontagne, D.; Yaghi, O. M. *Proc. Natl. Acad. Sci. U. S. A.* **2008**, *105*, 11623.
(4) Critoph, R. E. *Appl. Therm. Eng.* **1996**, *16*, 891.
(5) Tamainot-Telto, Z.; Metcalf, S. J.; Critoph, R. E.; Zhong, Y.; Thorpe, R. *Int. J. Refrig.* **2009**, *32*, 1212.
(6) Qajar, A.; Peer, M.; Andalibi, M. R.; Rajagopalan, R.; Foley, H. C. *Microporous Mesoporous Mater.* **2015**, *218*, 15.
(7) Katz, M. J.; Howarth, A. J.; Moghadam, P. Z.; DeCoste, J. B.; Snurr, R. Q.; Hupp, J. T.; Farha, O. K. *Dalton Trans.* **2016**, *45*, 4150.
(8) Petit, C.; Bandosz, T. J. *Adv. Funct. Mater.* **2010**, *20*, 111.
(9) Doonan, C. J.; Tranchemontagne, D. J.; Glover, T. G.; Hunt, J. R.; Yaghi, O. M. *Nat. Chem.* **2010**, *2*, 235.
(10) Van Humbeck, J. F.; McDonald, T. M.; Jing, X.; Wiers, B. M.; Zhu, G.; Long, J. R. *J. Am. Chem. Soc.* **2014**, *136*, 2432.
(11) Narayanan, S.; Yang, S.; Kim, H.; Wang, E. N. *Int. J. Heat Mass Transfer* **2014**, *77*, 288.
(12) Takahashi, A.; Tanaka, H.; Parajuli, D.; Nakamura, T.; Minami, K.; Sugiyama, Y.; Hakuta, Y.; Ohkoshi, S.-I.; Kawamoto, T. *J. Am. Chem. Soc.* **2016**, *138*, 6376.
(13) Choi, H. J.; Dincă, M.; Long, J. R. *J. Am. Chem. Soc.* **2008**, *130*, 7848.
(14) Choi, H. J.; Dincă, M.; Dailly, A.; Long, J. R. *Energy Environ. Sci.* **2010**, *3*, 117.
(15) Wade, C. R.; Corrales-Sanchez, T.; Narayan, T. C.; Dincă, M. *Energy Environ. Sci.* **2013**, *6*, 2172.
(16) Colombo, V.; Galli, S.; Choi, H. J.; Han, G. D.; Maspero, A.; Palmisano, G.; Masciocchi, N.; Long, J. R. *Chem. Sci.* **2011**, *2*, 1311.
(17) Liao, P.-Q.; Chen, H.; Zhou, D.-D.; Liu, S.-Y.; He, C.-T.; Rui, Z.; Ji, H.; Zhang, J.-P.; Chen, X.-M. *Energy Environ. Sci.* **2015**, *8*, 1011.
(18) Deng, H.; Grunder, S.; Cordova, K. E.; Valente, C.; Furukawa, H.; Hmadeh, M.; Gándara, F.; Whalley, A. C.; Liu, Z.; Asahina, S.; Kazumori, H.; O'Keeffe, M.; Terasaki, O.; Stoddart, J. F.; Yaghi, O. M. *Science* **2012**, *336*, 1018.
(19) Denysenko, D.; Grzywa, M.; Tonigold, M.; Streppel, B.; Krkljus, I.; Hirscher, M.; Mugnaioli, E.; Kolb, U.; Hanss, J.; Volkmer, D. *Chem. - Eur. J.* **2011**, *17*, 1837.
(20) Rosi, N. L.; Kim, J.; Eddaoudi, M.; Chen, B.; O'Keeffe, M.; Yaghi, O. M. *J. Am. Chem. Soc.* **2005**, *127*, 1504.
(21) Dietzel, P. D. C.; Panella, B.; Hirscher, M.; Blom, R.; Fjellvåg, H. *Chem. Commun.* **2006**, *1*, 959.
(22) Wang, T. C.; Bury, W.; Gómez-Gualdrón, D. A.; Vermeulen, N. A.; Mondloch, J. E.; Deria, P.; Zhang, K.; Moghadam, P. Z.; Sarjeant, A. A.; Snurr, R. Q.; Stoddart, J. F.; Hupp, J. T.; Farha, O. K. *J. Am. Chem. Soc.* **2015**, *137*, 3585.
(23) Brunauer, S.; Emmett, P. H.; Teller, E. *J. Am. Chem. Soc.* **1938**, *60*, 309.
(24) Barrett, E. P.; Joyner, L. G.; Halenda, P. P. *J. Am. Chem. Soc.* **1951**, *73*, 373.
(25) Kruk, M.; Jaroniec, M.; Sayari, A. *Langmuir* **1997**, *13*, 6267.
(26) Schaate, A.; Roy, P.; Godt, A.; Lippke, J.; Waltz, F.; Wiebcke, M.; Behrens, P. *Chem. - Eur. J.* **2011**, *17*, 6643.
(27) Morris, W.; Doonan, C. J.; Yaghi, O. M. *Inorg. Chem.* **2011**, *50*, 6853.
(28) Queen, W. L.; Bloch, E. D.; Brown, C. M.; Hudson, M. R.; Mason, J. A.; Murray, L. J.; Ramirez-Cuesta, A. J.; Peterson, V. K.; Long, J. R. *Dalt. Trans.* **2012**, *41*, 4180.

DOI: 10.1021/jacs.6b05723
J. Am. Chem. Soc. 2016, 138, 9401−9404